

## **Supporting Information**

### **A new two-dimensional luminescent Ag<sub>12</sub> cluster-assembled material and its catalytic activity for reduction of hexacyanoferrate (III)**

*Riki Nakatani,†<sup>a</sup> Sourav Biswas,†<sup>a</sup> Tsukasa Irie,<sup>a</sup> Jin Sakai,<sup>a</sup> Daisuke Hirayama,<sup>a</sup> Tokuhisa Kawawaki,<sup>a</sup> Yoshiki Niihori,<sup>b</sup> Saikat Das\*<sup>b</sup> and Yuichi Negishi\*<sup>a,b</sup>*

<sup>a</sup>Department of Applied Chemistry, Faculty of Science, Tokyo University of Science, Kagurazaka, Shinjuku-ku, Tokyo 162-8601, Japan.

<sup>b</sup>Carbon Value Research Center, Research Institute for Science & Technology, Tokyo University of Science, Tokyo 162-8601, Japan.

†These authors contributed equally.

\*Corresponding Authors

S.D.: saikatdas@rs.tus.ac.jp

Y.N.: negishi@rs.tus.ac.jp

## Table of Contents

Name	Description	Page No.
	General information	S3-S4
Table S1	Crystal data and structure refinement parameters of <b>TUS 3</b>	S5
Table S2	Time-correlated single-photon counting (TCSPC) measurement	S6
Table S3	Comparison of the catalytic activity	S6
Fig. S1	Optical microscope image of <b>TUS 3</b> crystals	S7
Fig. S2	Ag <sub>12</sub> core architecture	S8
Fig. S3	Topology of <b>TUS 3</b>	S9
Fig. S4	Separation distance between the layers in <b>TUS 3</b>	S10
Fig. S5	Presence of the solvent molecules inside the pores of <b>TUS 3</b>	S11
Fig. S6	BET plot for <b>TUS 3</b>	S12
Fig. S7	Pore size distribution for <b>TUS 3</b>	S13
Fig. S8	High resolution binding energy plot of each element obtained from the XPS measurement of <b>TUS 3</b>	S14
Fig. S9	TGA profile of <b>TUS 3</b>	S15
Fig. S10	Matched PXRD patterns of crystalline <b>TUS 3</b> crystals and even after water exposure	S16
Fig. S11	UV-Vis absorbance of <b>TUS 3</b> in water, NMP and linker in NMP	S17
Fig. S12	PL emission of <b>TUS 3</b> in solid-state	S18
Fig. S13	Effect of <b>TUS 3</b> in the reaction when 0.5 nM <b>TUS 3</b> was added	S19
Fig. S14	FT-IR spectra and PXRD of <b>TUS 3</b> and after different cycles of catalysis	S20
Fig. S15	HRTEM images of <b>TUS 3</b> before and after catalysis	S21
Fig. S16	EDS comparison of <b>TUS 3</b> as synthesized and after the 4 <sup>th</sup> cycle of catalysis	S22
	References	S23

## General information

### Reagents

All reagents and solvents were obtained from commercial suppliers and used as received, unless otherwise noted. Hexacyanoferrate (III) was purchased from Sigma-Aldrich. Sodium borohydride and *tert*-butyl mercaptan were provided by Tokyo Chemical Industry Co., Ltd. Silver trifluoroacetate (CF<sub>3</sub>COOAg) was provided by FUJIFILM Wako Pure Chemical Corporation. Silver nitrate (AgNO<sub>3</sub>), toluene, ethanol, acetonitrile, and methanol were purchased from Kanto Chemical Co., Inc. *N*-methyl-2-pyrrolidone (NMP) was purchased from Tokyo Chemical Industry Co., Ltd.

### Characterization

For the single-crystal X-ray diffraction (SCXRD) data collection, the single crystal was immersed in the cryoprotectant Parabar 10312 (Hampton Research, 34 Journey, Aliso Viejo, CA 92656-3317 USA) and mounted on a Dual-Thickness MicroMounts™ (MiTeGen, LLC, Ithaca, NY, USA). A Bruker D8 QUEST diffractometer was used to acquire the diffraction data for the single crystals using monochromated Mo K $\alpha$  radiation ( $\lambda = 0.71073 \text{ \AA}$ ). The crystal structure was resolved using Apex3 Bruker Software Suite.<sup>1</sup> Powder X-ray diffraction (PXRD) data were collected using a Rigaku X-ray diffractometer with Cu K $\alpha$  radiation ( $\lambda = 1.5418 \text{ \AA}$ ) operated at 40 kV and 40 mA. The data collection range was from  $2\theta = 5\text{-}30^\circ$  with a step size of  $0.02^\circ$  and scan speed of  $0.292^\circ$  per min. Nitrogen sorption isotherm measurements were conducted at 77 K with a Quantachrome's Quadrasorb evo gas sorption analyzer. The sample was degassed for 8 h at 50 °C prior to the adsorption measurements. The specific surface area was determined by the Brunauer–Emmett–Teller (BET) method within the relative pressure ( $P/P_0$ ) range of 0.02-0.1. The pore size distribution was evaluated from the adsorption data via the non-local density functional theory (NLDFT). Fourier transform infrared (FT-IR) spectra were collected on a JASCO FT/IR-4600 spectrometer using KBr pellets from 4000 to 400 cm<sup>-1</sup> with a resolution of 0.964233 cm<sup>-1</sup>. Thermogravimetric analysis (TGA) curve was recorded on a Bruker TG-DTA2010SA instrument under nitrogen atmosphere from room temperature to 800 °C with a heating rate of 10 °C min<sup>-1</sup> and nitrogen flow rate of 50 mL min<sup>-1</sup>. The optical

microscope images were acquired with an Olympus SZX7 stereo microscope. Scanning electron microscopy with energy-dispersive X-ray spectroscopy (SEM-EDS) analysis was tested on a JEOL JSM-7001F/SHL field emission scanning electron microscope with accelerating voltage of 15 kV. High-resolution transmission electron microscopy (HRTEM) images were obtained at 80 kV with a JEOL JEM-2100F microscope. X-ray photoelectron spectroscopy (XPS) experiments were performed on a JPS-9-1-MC electron spectrometer (JEOL, Tokyo, Japan). The X-rays from the Mg-K $\alpha$  line (1253.6 eV) were used for excitation and all the binding energies were referenced to the neutral C 1s peak at 290.6 eV. The UV-Vis absorption spectra were recorded on a JASCO V-770 spectrophotometer. The photoluminescence (PL) spectra were acquired using an Edinburgh Instruments (EI) FLS1000 spectrofluorometer, equipped with a continuous (450 W) xenon lamp. PL decay curves were measured according to a time-correlated single-photon counting (TCSPC) technique with a fluorescent lifetime spectrometer (FLS1000) under the excitation of 375 nm picosecond laser.

## Synthesis procedures

**Synthesis of silver *tert*-butylthiolate (AgS<sup>t</sup>Bu).** AgS<sup>t</sup>Bu was synthesized following the literature procedure.<sup>2,3</sup>

## Catalysis experiment

In order to investigate the catalytic activity, we conducted our study using solvents prepared in a deionized water medium with a pH of 7.1 at room temperature. For our experiments, we utilized stock solutions with specific concentrations. The stock solution of [K<sub>3</sub>Fe(CN)<sub>6</sub>] had a concentration of 10<sup>-3</sup> M, while NaBH<sub>4</sub> was prepared at a concentration of 10<sup>-2</sup> M. To begin the experiment, we measured a precise amount of the solution in a 3 mL cuvette. In order to ensure accurate results, we appropriately diluted the solution. Furthermore, we introduced **TUS 3** into the cuvette, adjusting the concentration to achieve the desired total volume. By following this meticulous procedure, we were able to effectively evaluate the catalytic activity under the specified conditions.

**Table S1.** Crystal data and structure refinement parameters of **TUS 3**.

Identification code	<b>TUS 3</b>
Empirical formula	$C_{114}H_{120}Ag_{12}F_{18}N_{18}O_{24}S_6$
CCDC number	2277175
Formula weight	3955.07
Temperature/K	273.15
Crystal system	trigonal
Space group	<i>R</i> -3
<i>a</i> /Å	24.1539(5)
<i>b</i> /Å	24.1539(5)
<i>c</i> /Å	20.9231(9)
$\alpha$ /°	90
$\beta$ /°	90
$\gamma$ /°	120
Volume/Å <sup>3</sup>	10571.4(6)
<i>Z</i>	3
$\rho_{\text{calc}}$ /g cm <sup>-3</sup>	1.862
$\mu$ /mm <sup>-1</sup>	1.809
F(000)	5832
Crystal size/mm <sup>3</sup>	0.24 × 0.22 × 0.2
Radiation	MoK $\alpha$ ( $\lambda$ = 0.71073)
2 $\theta$ range for data collection/°	2.177 to 29.535°
Index ranges	-32 ≤ <i>h</i> ≤ 31, -32 ≤ <i>k</i> ≤ 31, -27 ≤ <i>l</i> ≤ 28
Reflections collected	47476
Independent reflections	6329 [ <i>R</i> <sub>int</sub> = 0.0482]
Data/restraints/parameters	6329/628/352
Goodness-of-fit on <i>F</i> <sup>2</sup>	1.042
Final <i>R</i> indexes [ <i>I</i> ≥ 2 $\sigma$ ( <i>I</i> )]	<i>R</i> <sub>1</sub> = 0.0357, <i>wR</i> <sub>2</sub> = 0.088
Final <i>R</i> indexes [all data]	<i>R</i> <sub>1</sub> = 0.0441, <i>wR</i> <sub>2</sub> = 0.0962
Largest diff. peak/hole / e Å <sup>-3</sup>	1.639/-1.300

**Table S2.** Parameters obtained from time-correlated single-photon counting (TCSPC) measurement.

<b>Sample</b>	<b>Component</b>	<b><math>\tau</math> (ns)</b>	<b><math>A</math></b>	<b><math>f</math></b>
<b>TUS 3</b>	1	0.4943	0.856	0.552
	2	2.3917	0.144	0.448

Fitting parameter is 1.1370.  $\tau$  represents the lifetime of each individual component,  $A$  represents the amplitude, and  $f$  determines the fractional population of each component.

**Table S3.** Comparison of the catalytic activity by keeping the reaction conditions same.

<b>Sample</b>	<b>Half-life (<math>t_{1/2}</math>) (s)</b>
[AgS <sup>t</sup> Bu] <sub>n</sub>	No catalytic activity
Ag nanoparticles (~ 10 nm)	207
Au nanoparticles (~ 10 nm)	180
<b>TUS 3</b>	14

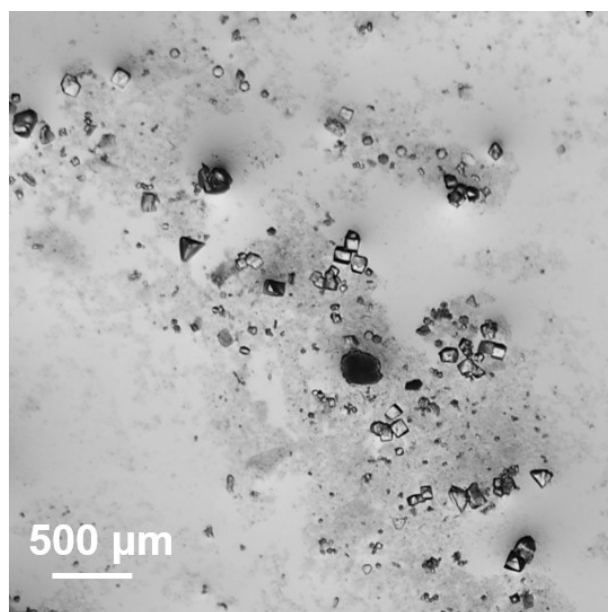


**Fig. S1** Optical microscope image of **TUS 3** crystals.

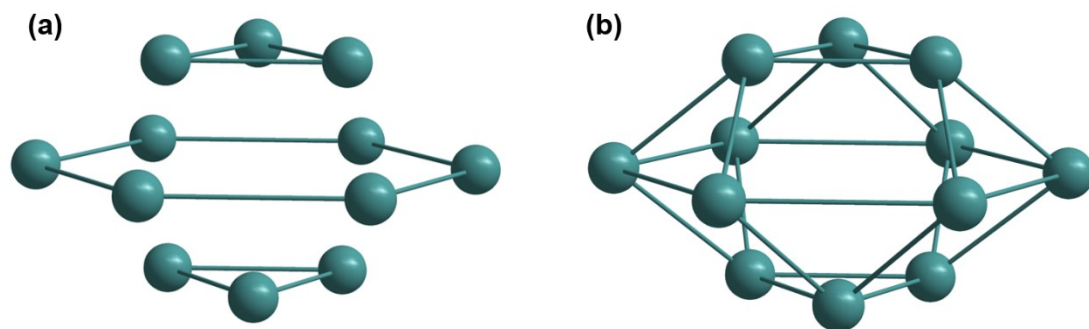


**Fig. S2** (a) Three different planes of Ag(I) atoms in  $\text{Ag}_{12}$  cluster node, (b) hollow cuboctahedron-like geometry of  $\text{Ag}_{12}$  when connecting all planes together.



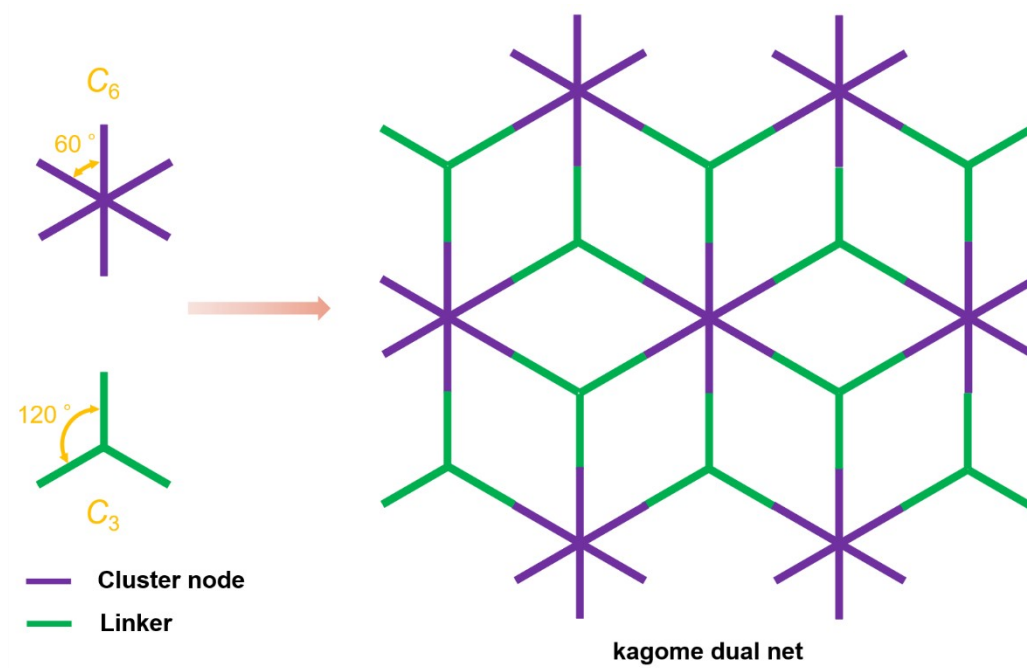


**Fig. S3** kgd (kagome dual) topology of TUS 3.

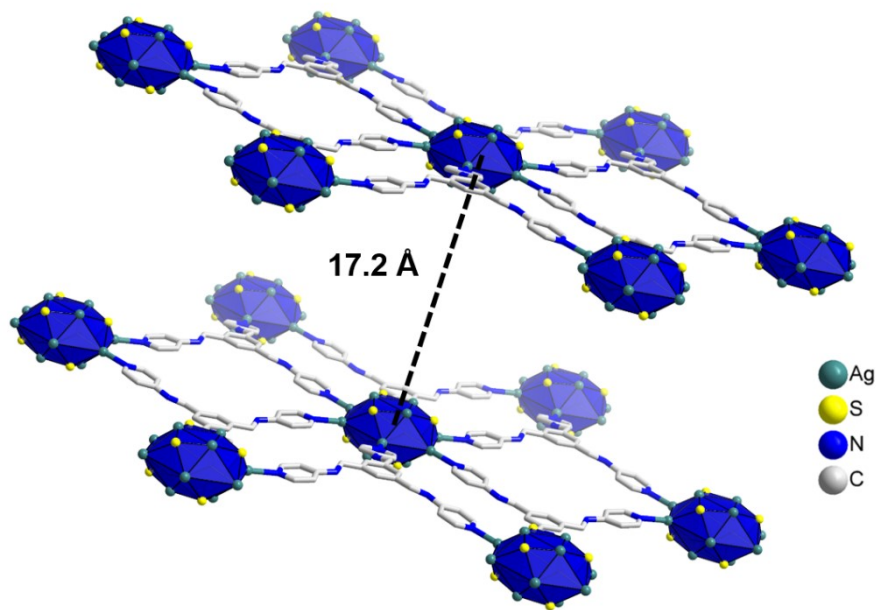


**Fig. S4** Separation distance between the layers in TUS 3.

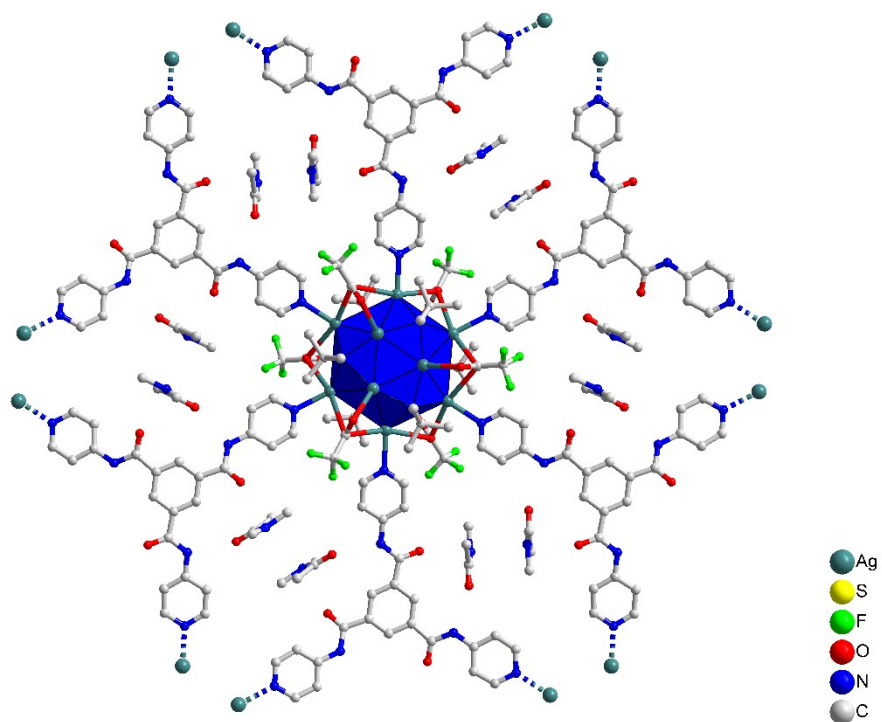


**Fig. S5** Presence of the solvent molecules inside the pores of **TUS 3** created by the linker molecules.

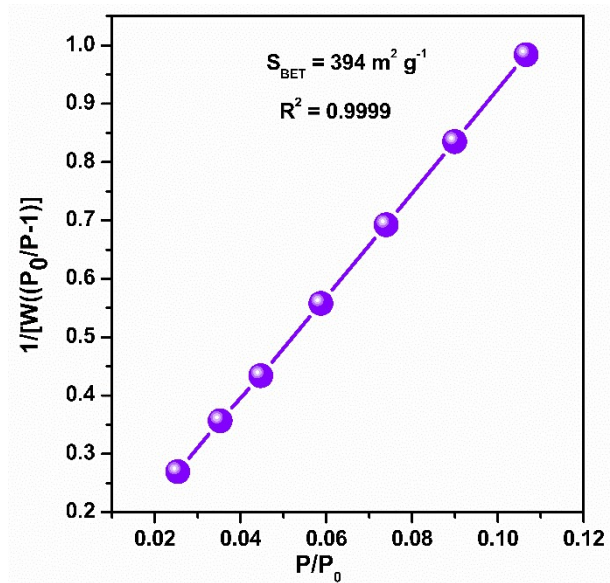


**Fig. S6** BET plot for TUS 3.

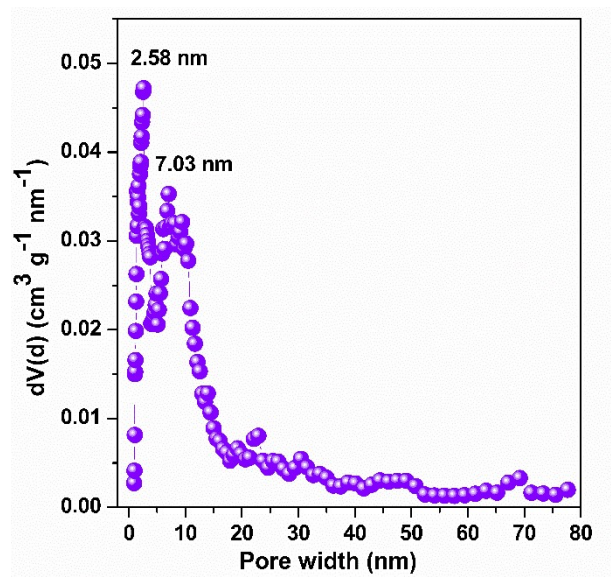


**Fig. S7** Pore size distribution for **TUS 3**.

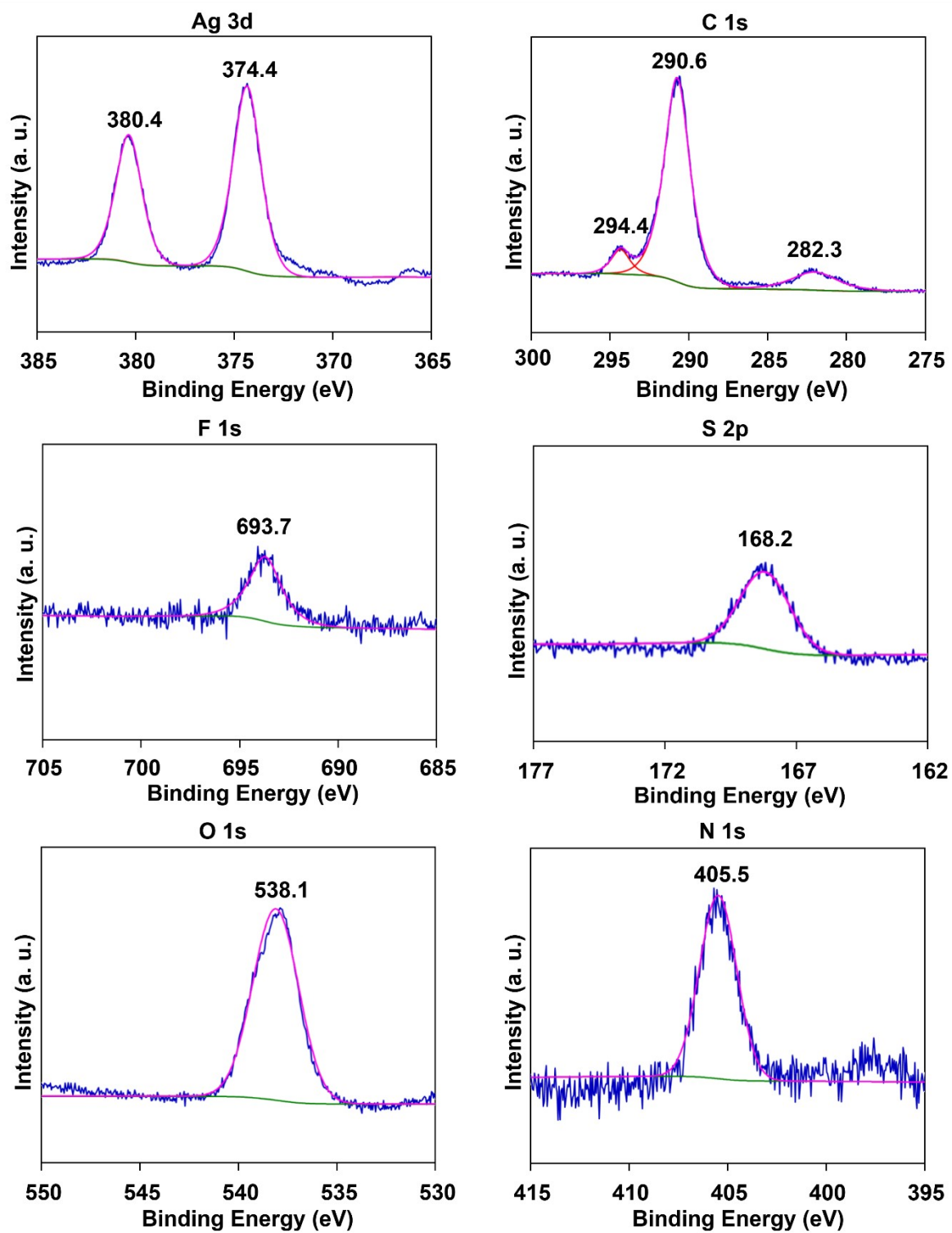


**Fig. S8** High resolution binding energy plot of each element obtained from the XPS measurement of TUS 3.

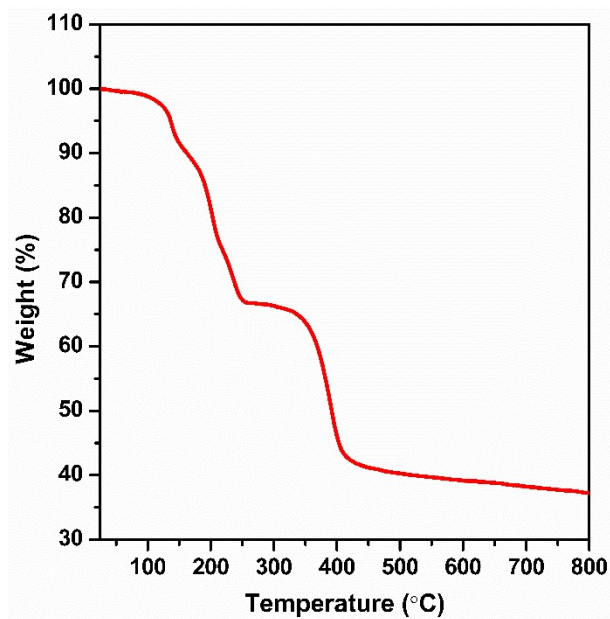


**Fig. S9** TGA profile of TUS 3 under N<sub>2</sub> atmosphere.

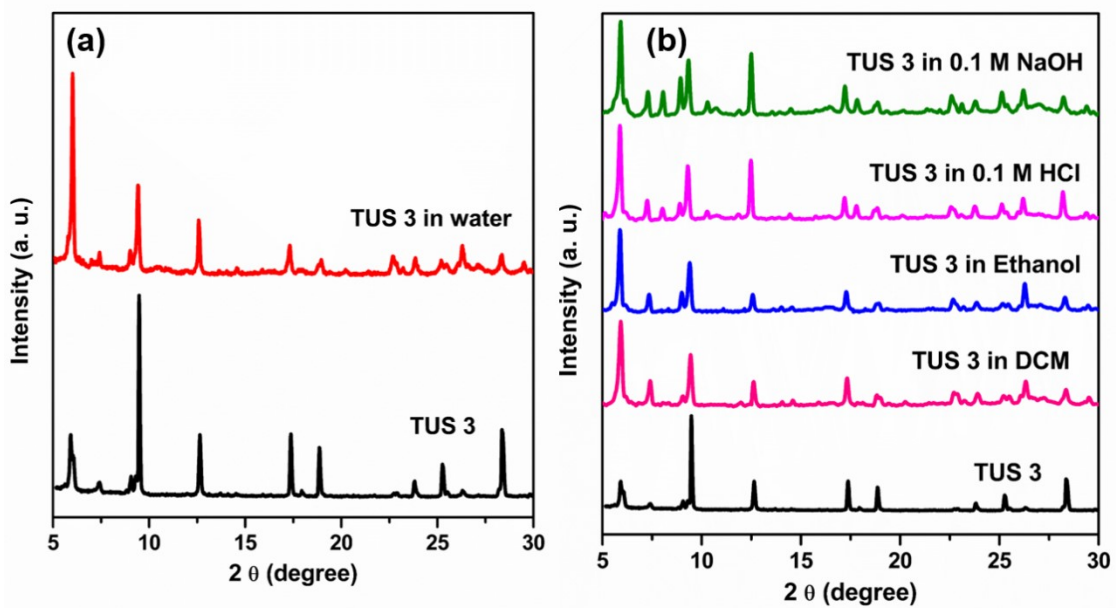


**Fig. S10** (a) Matched PXRD patterns of crystalline TUS 3 crystals and even after water exposure (b) PXRD patterns of TUS 3 after immersed in different solvent media.



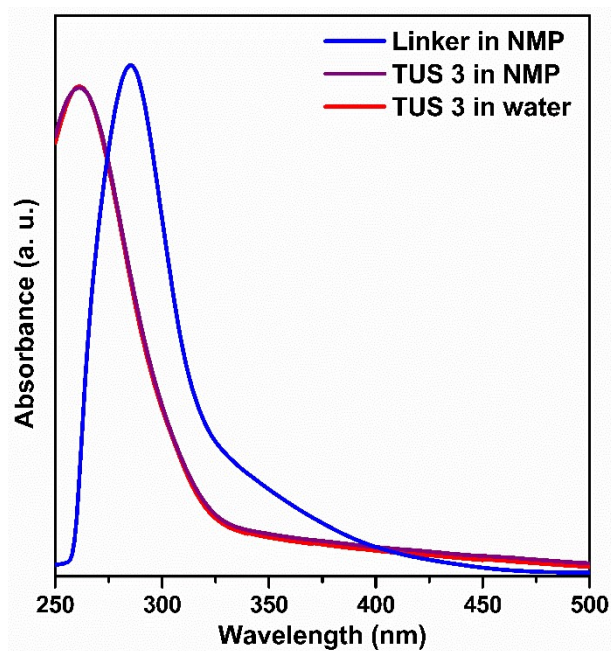


**Fig. S11** UV-Vis absorbance of **TUS 3** in water, NMP and linker in NMP.

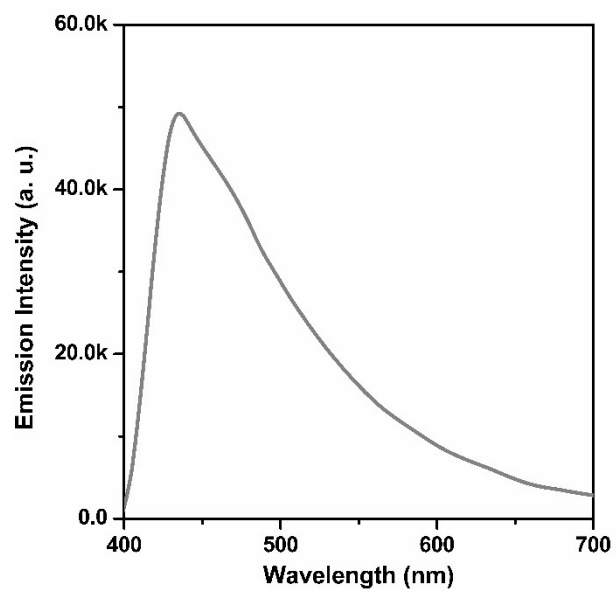


**Fig. S12** PL emission of **TUS 3** in solid-state.

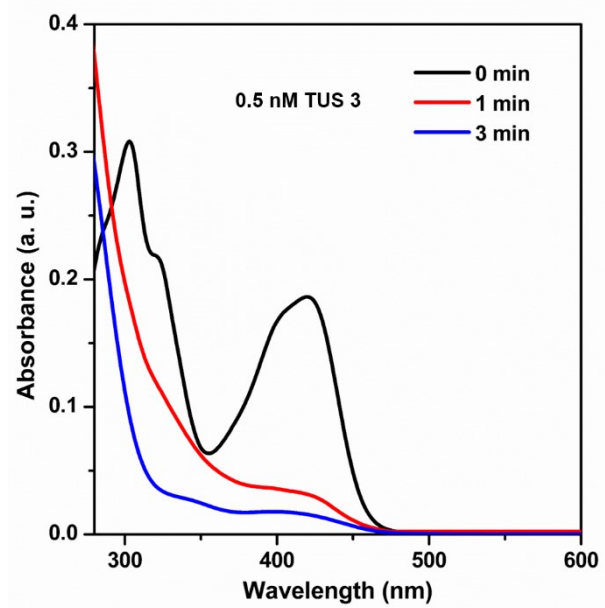


**Fig. S13** Effect of **TUS 3** in the reaction when 0.5 nM **TUS 3** was added.

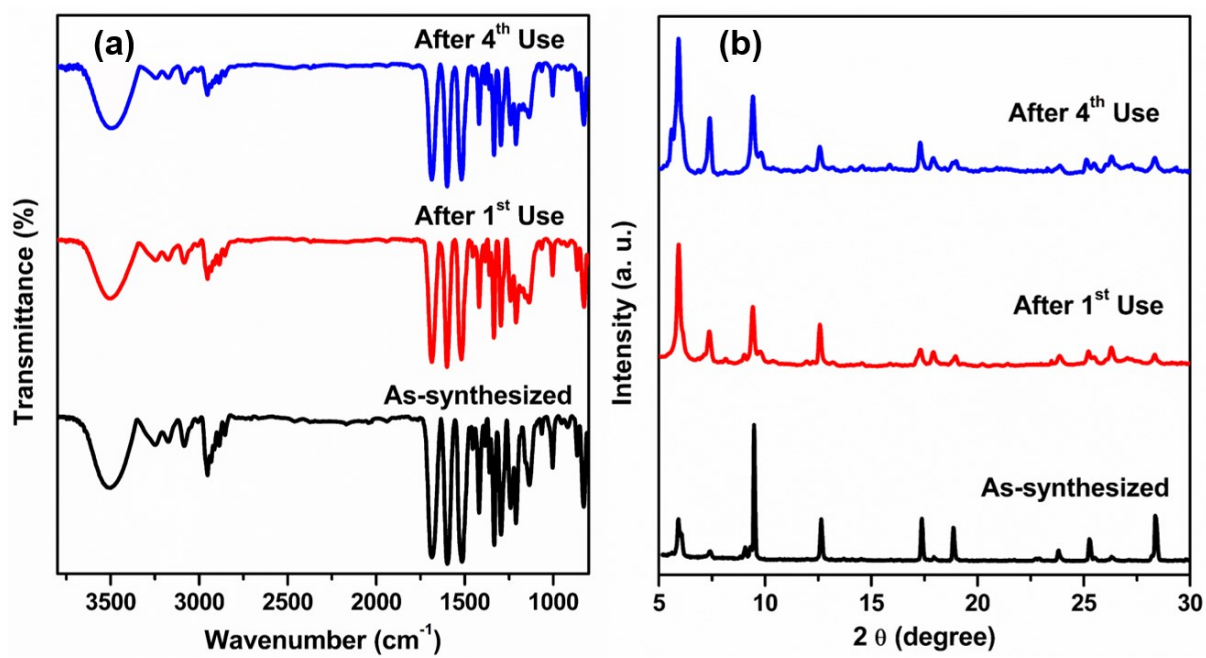


**Fig. S14** (a) FT-IR spectra and (b) PXRD patterns of TUS 3 and after different cycles of catalysis.

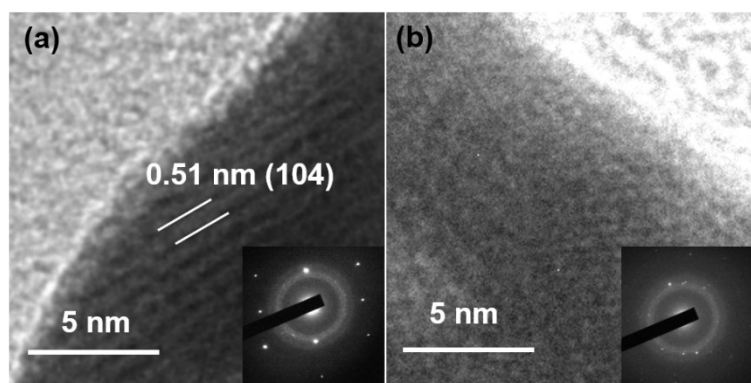


**Fig. S15** HRTEM image of **TUS 3** (a) before and (b) catalysis. The insets show the corresponding selected area electron diffraction (SAED) patterns. Lattice fringe correspond to (104) plane.

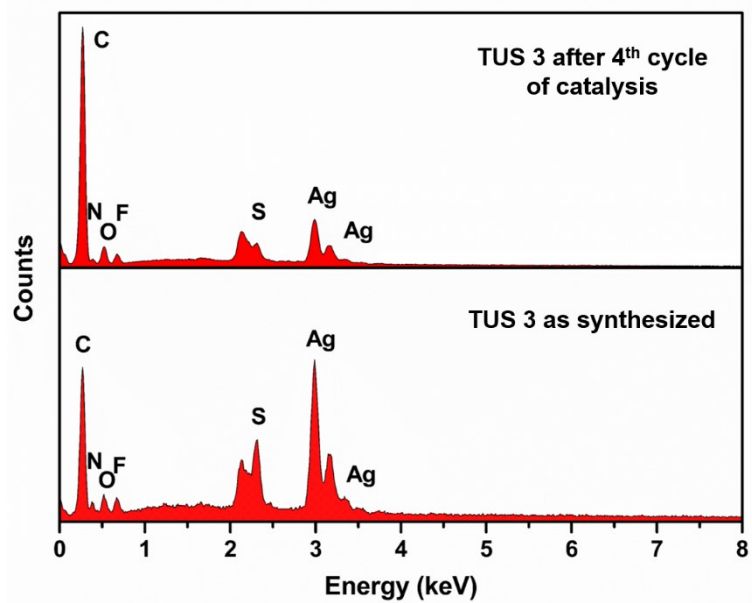


**Fig. S16** EDS comparison of **TUS 3** as synthesized and after the 4<sup>th</sup> cycle of catalysis.

## References

1. Bruker APEX3, v2019.1–0, Bruker AXS Inc., Madison, WI, USA, 2019.
2. B. K. Teo, Y. H. Xu, B. Y. Zhong, Y. K. He, H. Y. Chen, W. Qian, Y. J. Deng and Y. H. Zou, *Inorg. Chem.*, 2001, **40**, 6794-6801.
3. S. Das, T. Sekine, H. Mabuchi, S. Hossain, S. Das, S. Aoki, S. Takahashi and Y. Negishi, *Chem. Commun.*, 2023, **59**, 4000-4003.